

Identification of the thymidylate synthase within the genome of white spot syndrome virus

Qin Li,² Deng Pan,¹ Jing-hai Zhang² and Feng Yang¹

Correspondence
Feng Yang
mbiotech@public.xm.fj.cn

¹Key Laboratory of Marine Biogenetic Resources, Third Institute of Oceanography, SOA, 178 Daxue Road, Xiamen 361005, China

²Department of Biochemistry and Molecular Biology, School of Pharmaceutical Engineering, Shenyang Pharmaceutical University, Shenyang 110016, China

Received 19 February 2004
Accepted 11 March 2004

Thymidylate synthase (TS) (EC 2.1.1.45) is essential for the *de novo* synthesis of dTMP in prokaryotic and eukaryotic organisms. Within the white spot syndrome virus (WSSV) genome, an open reading frame (WSV067) that encodes a 289 amino acid polypeptide showed significant homology to all known TSs from species including mammals, plants, fungi, protozoa, bacteria and DNA viruses. In this study, WSV067 was expressed in *Escherichia coli*, and the purified recombinant protein showed TS activity in dUMP–folate-binding assays using ultraviolet difference spectroscopy. RT-PCR and Western blot analyses showed that WSV067 was a genuine and early gene. Phylogenetic analysis revealed that WSSV-TS was more closely related to the TSs of eukaryotes than to those from prokaryotes.

INTRODUCTION

White spot syndrome virus (WSSV) is a major pathogen that is mainly found in the cultivated shrimp. Although the determination of the WSSV genomic DNA sequence from three different isolates (GenBank accession nos AF332093, AF369029 and AF440570) has greatly facilitated the investigation of pathogenicity-related genes or gene products of WSSV, and some major structural proteins (Van Hulst *et al.*, 2001; Huang *et al.*, 2002; Zhang *et al.*, 2002) and enzymes (Tsai *et al.*, 2000; Van Hulst *et al.*, 2000; Chen *et al.*, 2002) have been identified, the interaction between WSSV and its host has still not been well defined. Thus there is an urgent need to study further virus gene products to clarify the infectious mechanism and discover potential therapeutic targets or methods for prevention and treatment of this disease.

Within the genome of WSSV, on the basis of the presence of highly conserved motifs, WSV067 encoding a putative thymidylate synthase (termed WSSV-TS) has been tentatively characterized (Yang *et al.*, 2001). It is located at position 31092–31958 bp in the genome and encodes a 289 aa protein (32.6 kDa).

Thymidylate synthase (TS) is essential for the *de novo* synthesis of deoxythymidine monophosphate (dTMP) in prokaryotic and eukaryotic organisms by catalysing the reductive methylation of 2'-deoxyuridylate (dUMP) by 5,10-methylenetetrahydrofolate to give dTMP and dihydrofolate. Consequently it plays a major role in the DNA replication of a cell or a DNA virus (Perryman *et al.*, 1986) and has been used successfully as a therapeutic target for

the treatment of proliferation diseases such as cancer (Danenbergh, 1977).

The catalytic mechanism of TS has been widely studied in the past, and much is known about the structure and function of the enzyme (Perry *et al.*, 1990). In protozoans and plants, TS combines with dihydrofolate reductase (EC 1.5.1.3) to form a bifunctional dihydrofolate reductase–TS (DHFR–TS). For DNA viruses, TS is only found in bacteriophage (Belfort *et al.*, 1983b; Kenny *et al.*, 1985), herpesvirus (Bodemer *et al.*, 1986; Richter *et al.*, 1988; Russo *et al.*, 1996) and three insect viruses including Chilo iridescent virus (*Invertebrate iridescent virus 6*; IRV6) (Muller *et al.*, 1998), *Melanoplus sanguinipes entomopoxvirus* (MSEV) (Afonso *et al.*, 1999) and *Heliothis zea* virus 1 (HzV-1) (Chen *et al.*, 2001).

In this work, homologous and phylogenetic analyses were performed to study the evolutionary relationship of WSSV-TS using known TS sequences in the SWISS-PROT database. The transcription and expression of WSSV-TS was identified with RT-PCR, rapid amplification of cDNA ends (RACE) and Western blot analyses. The WSSV recombinant TS protein (termed rTS) was expressed in *Escherichia coli* and was functionally identified by dUMP–folate-binding activity assay.

METHODS

Crayfish *Cambarus clarkii* infection with WSSV. The virus inoculum used for injections was extracted from diseased *Penaes japonicus* showing the prominent characteristic white spots, and which were collected from Xiamen, China. Tissues (muscle, heart

and gill) were homogenized in TNE buffer (20 mM Tris/HCl, 400 mM NaCl, 10 mM EDTA, pH 7.4) at 0.1 g ml⁻¹. After centrifugation at 3000 g for 10 min, the supernatant was filtered (0.45 µm filter) and injected intramuscularly into *C. clarkii* (collected from Anhui Province, China) in the lateral area of the fourth abdominal segment. At various stages [i.e. 0, 2, 4, 6, 12, 24, 48 and 72 h post-infection (h p.i.)], the hepatopancreas was freshly avulsed from the infected crayfish, frozen immediately in liquid nitrogen and kept there until use.

Homologous and phylogenetic analyses of WSSV-TS. The amino acid sequences of TS from mammals, fungi, bacteria, protozoa and DNA viruses in the SWISS-PROT databases were used in homologous and phylogenetic analyses. The homologous analysis was performed using DNAMAN software (Lynnon BioSoft). Amino acid sequences of TS from human (TYSY_HUMAN), mouse (TYSY_MOUSE), rat (TYSY_RAT), human herpesvirus 8 (TYSY_KSHV), herpesvirus saimiri (TYSY_HSVSA), equine herpesvirus type 2 (TYSY_SHVE2), herpesvirus atele (TYSY_SHVAT), varicella-zoster virus (TYSY_VZVD), fruitfly (TYSY_DROME), mushroom (TYSY_AGABI), baker's yeast (TYSY_YEAST), HzV-1 (TYSY_HzV-1), IRV6 (TYSY_IRV6), MSEV (TYSY_MSEV), *Escherichia coli* (TYSY_ECOLI), bacteriophage T4 (TYSY_BPT4), *Crithidia fasciculata* (DRTS_CRIFA), carrot (DRTS_DAUCA) and soybean (DRTS_SOYBN) were used in the multiple sequence alignment (Table 1).

Phylogenetic analysis was performed using DNAMAN to produce input files of aligned protein sequences. A phylogenetic tree was drawn to investigate the evolutionary position of WSSV-TS.

Transcriptional analysis of gene. Total RNAs, extracted from the hepatopancreas of WSSV-infected crayfish at different times after infection (i.e. 0 to 72 h p.i.), were treated with DNase and reverse-transcribed. The cDNAs were subjected to PCR using *ts*-specific forward and reverse primers (5'-Ttaaccatcatcaatg-3', 5'-cagcgattaccattctag-3'). The PCR cycles were as follows: 94 °C for 2 min, 30 cycles of 94 °C for 30 s, 58 °C for 30 s, 72 °C for 1 min, followed by an elongation at 72 °C for 10 min. The crayfish β-actin gene was used as the internal control for RT-PCR with a gene-specific primer set (5'-TCATCAGGGTGTGATGGT-3' and 5'-TCTGAGTCATCTTCTCAC-3'). Total RNA from healthy crayfish was used as the negative control.

RACE. Based on the nucleotide sequence of WSV067, the 5' and 3' ends of the cDNA encoding WSSV-TS were obtained by 5'- and 3'-RACE using a commercial 5'/3'-RACE kit (Roche), according to the manufacturer's recommendations. The RNA samples used in this study were extracted from WSSV-infected crayfish 24 h p.i. and then treated with RNase-free DNase. For 5'-RACE, the first strand cDNA was synthesized using the *ts*-specific primer TSp1 (5'-CACAACTCCTCTCCAGAAAAT-3') and then a poly(A) tail was added to the cDNA products using terminal transferase in the presence of dATP. The primer TSp2 (5'-GGTAGTGAGAACTGGAATAGT-3') and an oligo(dT) anchor primer supplied with the kit were used for PCR. For 3'-RACE, first-strand cDNA was synthesized using an oligo(dT) anchor primer. The primer TSp3 (5'-GAGGGAGAACATCAATATTTG-3') and an anchor primer supplied with the kit were used for PCR. The PCR products from 5'- and 3'-RACE were each purified on a 1.5% agarose gel and subcloned into the pMD18-T vector (TaKaRa). Arbitrarily selected clones were sequenced and compared with the genomic DNA sequence of WSSV.

Expression and purification of His-tagged WSSV-TS in *E. coli*. The WSSV-*ts* gene was amplified from WSSV genomic DNA using the forward primer (5'-AGTCGGATCCGAGGGAGAA-CATCA-3') and the reverse primer (5'-ACTGAAGCTTCCTTAA-CATGATTC-3') that contained recognition sequences for *Bam*HI and *Hind*III restriction enzymes (underlined). The amplicon was

cloned into the pQE30 vector (Qiagen). The recombinant plasmid was transformed into *E. coli* BL21(DE3) cells. Liquid cultures were grown in a shaking incubator (200 r.p.m.) at 37 °C until the OD₆₀₀ reached 0.5 and these were then induced with 0.5 mM IPTG for 8 h at 28 °C. The cells were harvested by centrifugation at 4000 g for 5 min. The recombinant WSSV-TS (termed *r*TS) was purified by Ni-NTA affinity chromatography under native conditions following methodology in the *QIAexpressionist* handbook (Qiagen). The *E. coli* cells containing pQE30 vector were also induced with IPTG and total protein extracts were applied to the Ni-NTA column as described above. Final eluates were collected and used as the negative control (termed NC).

Preparation of antibody. The purified *r*TS was used as an antigen to immunize mice by intradermal injection once every 10 days. Antigen (100 µg) was mixed with an equal volume of Freund's complete adjuvant (Sigma) for the first injection. The subsequent three injections were conducted using 100 µg antigen mixed with an equal volume of Freund's incomplete adjuvant. Four days after the last injection, mice were exsanguinated and the antisera were collected. The antiserum titres were determined by ELISA using horseradish peroxidase-conjugated goat anti-mouse IgG (Promega). For a negative control, antigen was replaced with 1 × PBS.

Western blot. Total proteins, extracted from hepatopancreas of infected crayfish at various times (i.e. 0, 2, 4, 6, 12, 24, 48 and 72 h p.i.), were separated by SDS-PAGE. These proteins were transferred onto a PVDF membrane (Amersham Pharmacia). The membrane was then immersed in blocking buffer (2% BSA, 20 mM Tris, 150 mM NaCl, 0.1% Tween 20, pH 7.5) at room temperature for 30 min, followed by incubation with anti-*r*TS serum (diluted 1:2000) for 1 h. Following this, alkaline phosphatase-conjugated goat anti-mouse IgG (Promega) was used as the secondary antibody. Detection was performed using Western Blue Stabilized Substrate for Alkaline Phosphatase (Promega).

UV difference spectroscopy analysis. This was performed as described (Lockshin *et al.*, 1984). In brief, 5 µl of 0.424 mM dUMP was added to 500 µl buffer (50 mM TES pH 7.4, 25 mM MgCl₂, 1.0 mM EDTA, 5.0 mM DTT) containing 5 µl purified *r*TS and 10 µl of 36.6 µM folate (Sigma). The reaction was conducted in a sample cuvette at room temperature in a spectrophotometer thermostatic chamber. The absorbance was recorded within the 250–360 nm range and the final difference spectra, representing the *r*TS-dUMP-folate complex, were obtained. In the negative control, the same dUMP dose was added to the sample cuvette containing the same buffer but substituting the NC fraction mentioned above.

RESULTS

Multiple sequence alignment and evolutionary position of WSSV-TS

Amino acid sequences of 20 TS or DHFR-TS from mammals, yeasts, bacteria, DNA viruses, protozoa and plants were used for the multiple sequence alignment. The results showed that there was significant homology with five conserved motifs including the folate-binding site (Chiericatti & Santi, 1998) (Fig. 1, motif 1), catalytic centre region (Carreras & Santi, 1995) (Fig. 1, motif 2), dUMP-binding site (Tong, 1998) (Fig. 1, motif 3) and proton transportation region (Carreras & Santi, 1995) (Fig. 1, motif 4). These motifs are essential for the biofunction of TS (Carreras & Santi, 1995). The consensus sequence GDLGPVYGFQWRHFGA (Fig. 1, motif 5) was highly

Table 1. Information on TS sequences compared

Forty-two TS amino acid sequences, from prokaryotic and eukaryotic organisms including mammals, fungi, bacteria, protozoa and DNA viruses, were used in homologous and phylogenetic analyses. The accession numbers of each of the TS sequences and their similarity to WSSV-TS are also indicated in the table.

TS	Species	Organism	Accession no.	Reference	Evolutional origin	Similarity (%)
WSSV-TS	Whispovirus	<i>Nimaviridae</i>	–	Yang <i>et al.</i> (2001)	–	100
TYSY_HUMAN	<i>Homo sapiens</i>	Mammal	P04818	Kaneda <i>et al.</i> (1990)	Eukaryote	63·6
TYSY_MOUSE	<i>Mus musculus</i>	Mammal	P07607	Perryman <i>et al.</i> (1986)	Eukaryote	62·9
TYSY_DROME	<i>Drosophila melanogaster</i>	Insect	O76511	Adams <i>et al.</i> (2000)	Eukaryote	58·7
TYSY_KSHV	<i>Human herpesvirus 8</i>	<i>Herpesviridae</i>	P90463	Russo <i>et al.</i> (1996)	Eukaryote	61·5
TYSY_HSVSA	Herpesvirus saimiri	<i>Herpesviridae</i>	P06854	Honess <i>et al.</i> (1986)	Eukaryote	61·2
TYSY_HSVE2	Equine herpesvirus type 2	<i>Herpesviridae</i>	Q89940	Telford <i>et al.</i> (1995)	Eukaryote	59·4
TYSY_HSVAT	Herpesvirus ateles	<i>Herpesviridae</i>	P12462	Richter <i>et al.</i> (1988)	Eukaryote	59·4
TYSY_VZVD	Varicella-zoster virus	<i>Herpesviridae</i>	P09249	Davison & Scott (1986)	Eukaryote	57·3
DRTS_TRYBB	<i>Trypanosoma brucei brucei</i>	Protozoa	Q27783	Gamarro <i>et al.</i> (1995)	Eukaryote	64·2
DRTS_TRYCR	<i>Trypanosoma cruzi</i>	Protozoa	Q27793	Reche <i>et al.</i> (1994)	Eukaryote	60·8
DRTS_LEIAM	<i>Leishmania amazonensis</i>	Protozoa	P16126	Nelson <i>et al.</i> (1990)	Eukaryote	60·1
DRTS_LEIMA	<i>Leishmania major</i>	Protozoa	P07382	Beverley <i>et al.</i> (1986)	Eukaryote	58·7
DRTS_PARTE	<i>Paramecium tetraurelia</i>	Protozoa	Q27828	Schlichtherle <i>et al.</i> (1996)	Eukaryote	54·6
DRTS_CRIFA	<i>Crithidia fasciculata</i>	Protozoa	Q23695	Hughes <i>et al.</i> (1989)	Eukaryote	54·2
DRTS_TOXGO	<i>Toxoplasma gondii</i>	Protozoa	Q07422	Roos (1993)	Eukaryote	53·5
DRTS_PLACH	<i>Plasmodium chabaudi</i>	Protozoa	P20712	Cheng & Saul (1994)	Eukaryote	52·4
DRTS_PLABA	<i>Plasmodium berghei</i>	Protozoa	Q27713	van Dijk <i>et al.</i> (1994)	Eukaryote	51·7
DRTS_PLAVI	<i>Plasmodium vivax</i>	Protozoa	O02604	Eldin de Pecoulas <i>et al.</i> (1998)	Eukaryote	51·3
DRTS_MAIZE	Maize	Plant	O81395	Cox <i>et al.</i> (1999)	Eukaryote	58·7
DRTS_SOYBN	Soybean	Plant	P51820	Wang <i>et al.</i> (1995)	Eukaryote	58·4
DRTS_DAUCA	Carrot	Plant	P45350	Luo <i>et al.</i> (1993)	Eukaryote	57·3
TYSY_YEAST	<i>Saccharomyces cerevisiae</i>	Fungi	P06785	Taylor <i>et al.</i> (1987)	Eukaryote	56·5
TYSY_CANAL	<i>Candida albicans</i>	Fungi	P12461	Singer <i>et al.</i> (1989)	Eukaryote	53·3
TYSY_AGABI	<i>Agaricus bisporus</i>	Fungi	Q9P4T7	Eastwood <i>et al.</i> (2000)	Eukaryote	50·8
TYSY_IRV6	Invertebrate iridescent virus 6	<i>Iridoviridae</i>	NP_149688	Muller <i>et al.</i> (1998)	Eukaryote	50·3
TYSY_MSEV	<i>Melanoplus sanguinipes</i> entomopoxvirus	<i>Poxviridae</i>	NP_048309	Afonso <i>et al.</i> (1999)	Eukaryote	50·2
TYSY_HZ-1	<i>Heliothis zea</i> virus 1	Unclassified virus	NP_690528	Chen <i>et al.</i> (2001)	Eukaryote	56·4
TYSY_ASCSU	<i>Ascaris suum</i>	Nematode	O96650	Tian & Tam (1998)	Eukaryote	56·1
TYSY_BRUME	<i>Brucella melitensis</i>	Bacteria	Q8YI37	Ivanova <i>et al.</i> (2002)	Prokaryote	49·2
TYSY_CAUCR	<i>Caulobacter crescentus</i>	Bacteria	Q9A6H0	Nierman <i>et al.</i> (2001)	Prokaryote	48·5
TYSY_COREF	<i>Corynebacterium efficiens</i>	Bacteria	Q8FR47	Nishio <i>et al.</i> (2003)	Prokaryote	48·4
TYSY_BACAA	<i>Bacillus anthracis</i>	Bacteria	Q81R23	Read <i>et al.</i> (2003)	Prokaryote	47·6
TYSY_BACCR	<i>Bacillus cereus</i>	Bacteria	Q81E05	Ivanova <i>et al.</i> (2003)	Prokaryote	47·6
TYSY_BUCAI	<i>Buchnera aphidicola</i> (<i>Acyrtosiphon pisum</i>)	Bacteria	P57515	Shigenobu <i>et al.</i> (2000)	Prokaryote	47·3
TYSY_ECOLI	<i>Escherichia coli</i>	Bacteria	P00470	Belfort <i>et al.</i> (1983a)	Prokaryote	46·5
TYSY_BUCAP	<i>Buchnera aphidicola</i> (<i>Schizaphis graminum</i>)	Bacteria	Q8K9C3	Tamas <i>et al.</i> (2002)	Prokaryote	45·3
TYSY_BUCBP	<i>Buchnera aphidicola</i> (<i>Baizongia pistaciae</i>)	Bacteria	P59427	Van Ham <i>et al.</i> (2003)	Prokaryote	44·9
TYSY_CLOAB	<i>Clostridium acetobutylicum</i>	Bacteria	Q97EV3	Noelling <i>et al.</i> (2001)	Prokaryote	35·6
TYSY_BACMO	<i>Bacillus mojavensis</i>	Bacteria	Q9ANR7	Edgell & Shub (2001)	Prokaryote	34·3
TYSY_BPT4	Bacteriophage T4	Bacteriophage	P00471	Belfort <i>et al.</i> (1983b)	Prokaryote	40·6
TYSY_BPPHT	Bacteriophage phi-3T	Bacteriophage	P07606	Kenny <i>et al.</i> (1985)	Prokaryote	33·9

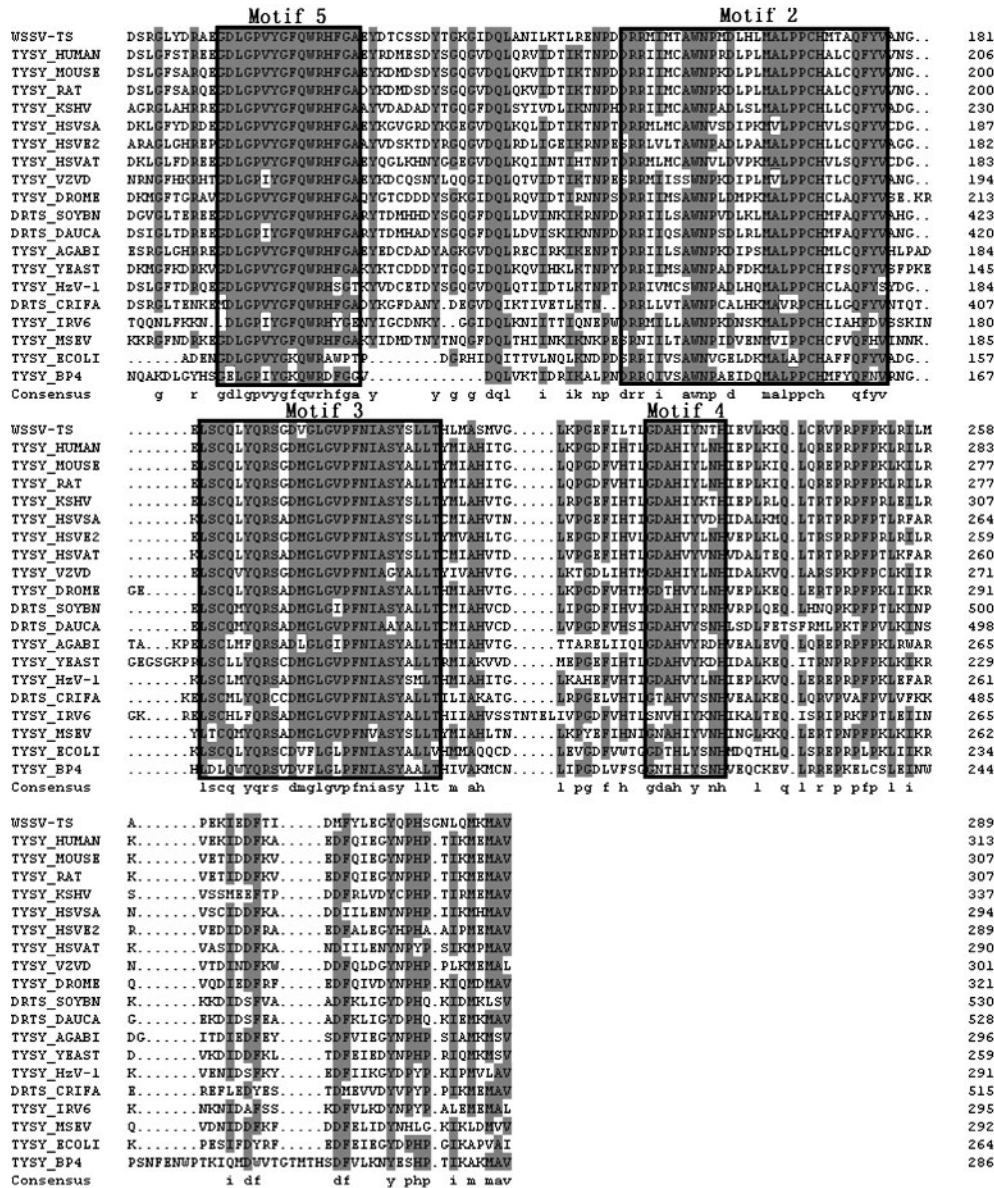


Fig. 1. Comparison of the amino acid sequences of TSs from eukaryotic and prokaryotic species. Published TS and DHFR-TS sequences were aligned with that of WSSV-TS; see Methods for abbreviations. The numbers at the right end of each row indicate the amino acid positions. Motif 1, folate-binding site; Motif 2, catalytic centre region; Motif 3, dUMP-binding site; Motif 4, proton transportation region; Motif 5, function undefined.

the highest similarity to DRTS_TRYBB (64.2%) and TYSY_HUMAN (63.6%) and the lowest similarity to TYSY_BACMO (34.3%) and TYSY_BPPHT (33.9%) (see Table 1). The similarity of WSSV-TS to TS from eukaryotes (50.2–64.2%) was higher than those from prokaryotes (33.9–49.2%). Its phylogenetic position indicated that WSSV-TS had the closest evolutionary relationship to the TS from parasitic protozoa of insects, and the furthest relationship to TS from bacteria and bacteriophage (Fig. 2), which was identical to what was found for the homology analysis results.

Mapping of the 5' and 3' ends of the WSSV-TS transcripts

The 5'-RACE products formed a single 150 bp band (Fig. 3a). Sequencing analysis of the products revealed that the 5' terminus was located 22 nt upstream of the predicted initiation codon (Fig. 3c), and a putative TATA box was found at 28 nt upstream of the transcriptional initiation sites. The sequence either side of the putative translation initiation codon (AATATGG) complied with the Kozak rule (Kozak, 1989).

The 3'-RACE fragments (Fig. 3b) were also cloned and sequenced. Although there was no typical polyadenylation signal (AATAAA), a poly(A) tail was added 116 nt downstream of the termination codon. This result indicated that other undefined signal pathways that regulate WSSV-*ts* polyadenylation may exist. The consensus sequence CGT-GTTAG, which was identical to the mRNA polyadenylation-related signal (PyGTGTTPyPy) of herpesvirus (McLauchlan *et al.*, 1985), was present at 19 nt upstream of the poly(A) tail (Fig. 3c).

Expression of WSSV-*ts* in *E. coli*

For the convenience of protein purification and identification, full-length WSSV-TS was expressed in *E. coli* as a fusion protein with an N-terminal His tag. The induced (plus IPTG at 37 °C) and non-induced samples were analysed by 14 % SDS-PAGE (Fig. 4a). A band (about 32 kDa) corresponding to *r*TS protein was observed in the induced sample when compared to the sample without induction. The soluble *r*TS was purified by Ni-NTA affinity chromatography under native conditions, and was found to match

the theoretical molecular mass of 32.6 kDa. Purified *r*TS was used for antibody preparation and the identification of function.

Transcription and expression analyses of WSSV-*ts* *in vivo*

RT-PCR was performed to detect *ts*-specific transcripts at different infection stages (0 to 72 h p.i.). The WSSV-*ts* transcript was first, slightly, detected at 4 h p.i. and maximally at 24 h p.i.; consequently, it was considered an early transcriptional gene of the WSSV genome. The WSSV-*ts* transcriptional pattern was similar to some other early WSSV genes (Van Hulten *et al.*, 2000; Tsai *et al.*, 2000; Chen *et al.*, 2002). When RNA was treated with RNase and then subjected to RT-PCR with *ts*-specific primers, no RT-PCR amplicon was seen, indicating that no virus genomic DNA was left in the prepared RNA (data not shown).

To investigate expression of WSSV-*ts* *in vivo*, samples extracted at various times up to 72 h p.i. from hepatopancreas of infected crayfish were analysed by Western

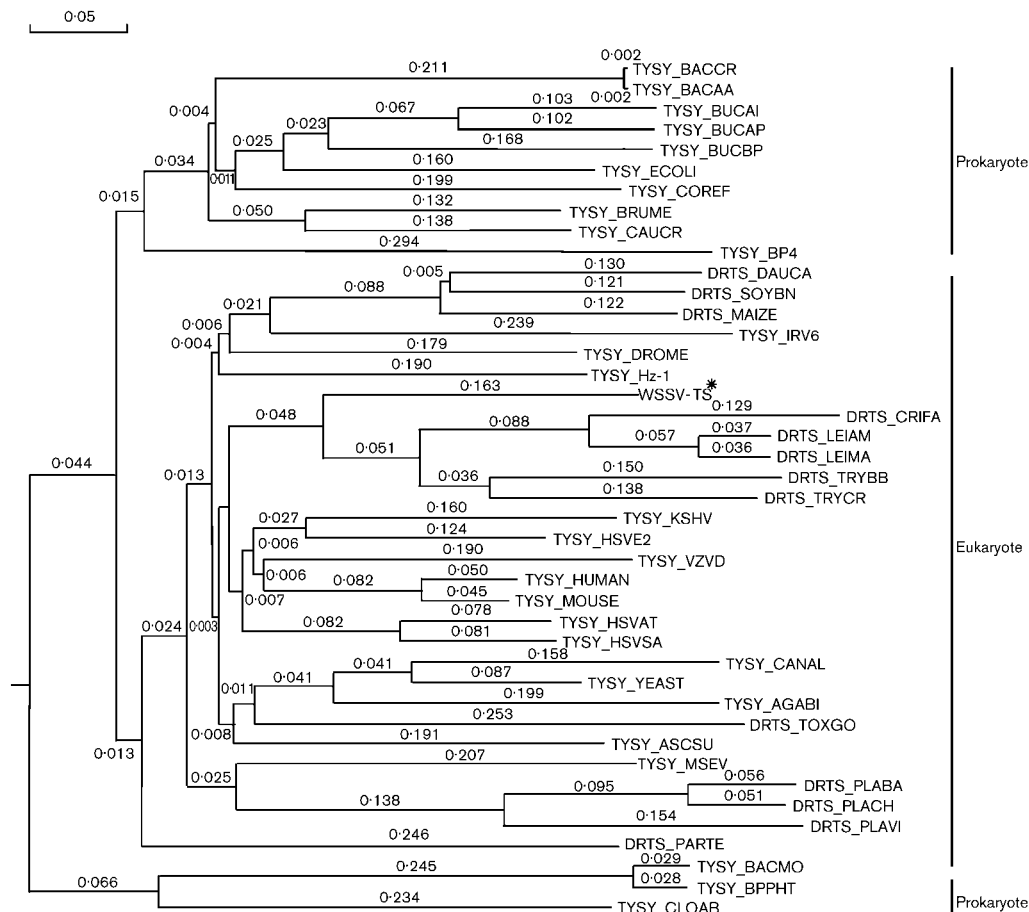


Fig. 2. Phylogenetic analysis of WSSV-TS performed using 27 TSs and 15 DHFR-TSs from different organisms including mammals, fungi, bacteria, protozoa and DNA viruses. The phylogenetic tree was drawn using DNAMAN software. WSSV-TS (indicated with *) grouped more closely to DHFR-TSs from protozoa than to those from other organisms.

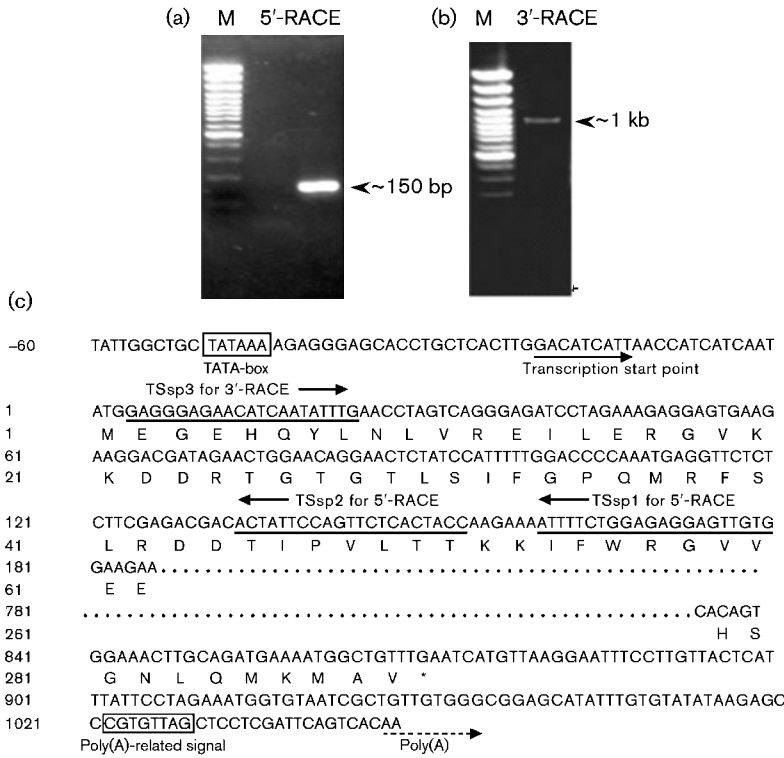


Fig. 3. Mapping of the 5' and 3' ends of the WSSV-ts transcript. (a) Agarose gel analysis of the 5'-RACE product; (b) agarose gel analysis of the 3'-RACE product. Lane M is a 100 bp ladder DNA marker (Takara). (c) Primers used for 5'/3'-RACE (TSsp1, TSsp2, TSsp3) are underlined. The predicted TATA box and poly(A)-related signal are boxed. The transcription start point, identified by 5'-RACE, is indicated with a solid line with arrows. The position of the poly(A) revealed by 3'-RACE is indicated by dashed lines with arrows.

blotting. An apparent band (about 32 kDa) corresponding to the theoretical molecular mass of WSSV-TS (32.6 kDa) was observed (Fig. 4b). WSSV-TS was first detected at 6 h p.i., maximally at 12 h p.i. and remained fairly constant thereafter. This result, fairly consistent with that of RT-PCR, suggested that WSSV-ts was a genuine and early virus gene.

dUMP-folate-binding activity assay

As shown in Fig. 4(c), the UV difference spectra, which were obtained following addition of dUMP to a buffer containing rTS and folate, revealed two maximum absorbances at 263 nm and 322 nm and a minimum absorbance at 295 nm. These are characteristic of typical dUMP-TS-folate complexes, and A_{322} increased linearly with the increased dUMP concentration. Since the function-related motifs in TS from different origins are all highly conserved, it was essential to rule out any influence of contamination from *E. coli* TS during rTS purification. In the negative control, only one maximum absorbance at 263 nm was detectable (Fig. 4d) suggesting that there was no interference due to contaminating TS from *E. coli* and that the UV difference spectrum results were reliable. The kinetic data obtained by spectroscopic analysis indicated that the K_m of dUMP was $4.7 \pm 0.5 \mu\text{M}$ and that the K_m of folate was $7.6 \pm 0.3 \mu\text{M}$.

DISCUSSION

WSSV is a major pathogen with a broad host range, high infectivity and causes high mortality. Approximately 181

open reading frames (ORFs) have been revealed by analysing the genomic DNA sequence and nearly 20% of them, including WSV067, are found without a typical polyadenylation signal (AATAAA) downstream of the ORFs (Yang *et al.*, 2001). Results from the transcriptional analysis showed that WSSV-ts mRNA was indeed polyadenylated, although the polyadenylation pathway is still not well defined. The consensus sequence (CGTGTAG), which is required for efficient formation and processing of poly(A) tails in 67% of mammalian mRNA 3' termini (McLauchlan *et al.*, 1985), is presumed to contribute to this unknown signal pathway. However, our findings provide the first example that WSSV genes without the typical polyadenylation signals could be polyadenylated using another poly(A) signal pathway during their transcription.

It has been reported that dUMP and folate are attached to the highly conserved TS binding sites to form a ternary complex during the catalytic reactions. The major amino acid residues for which a functional role has been reported are present within these binding sites. X-ray analysis of the TS crystal structure reveals that several key residues found in these motifs are essential for this reaction (Carreras & Santi, 1995). For instance in *E. coli* TS, the residues N¹⁷⁷ and Y¹⁸¹, which are located in a consensus sequence PFNIASY of the dUMP-binding site (motif 3), are involved in determining pyrimidine specificity and in dUMP-binding activity (Hardy & Nalivaika, 1992; Schiffer *et al.*, 1995). In addition, the aspartate residue (D²²¹) in human TS, in the consensus sequence DMGLGVP in motif 3, is involved in folate cofactor binding and catalysis (Chiericatti & Santi,

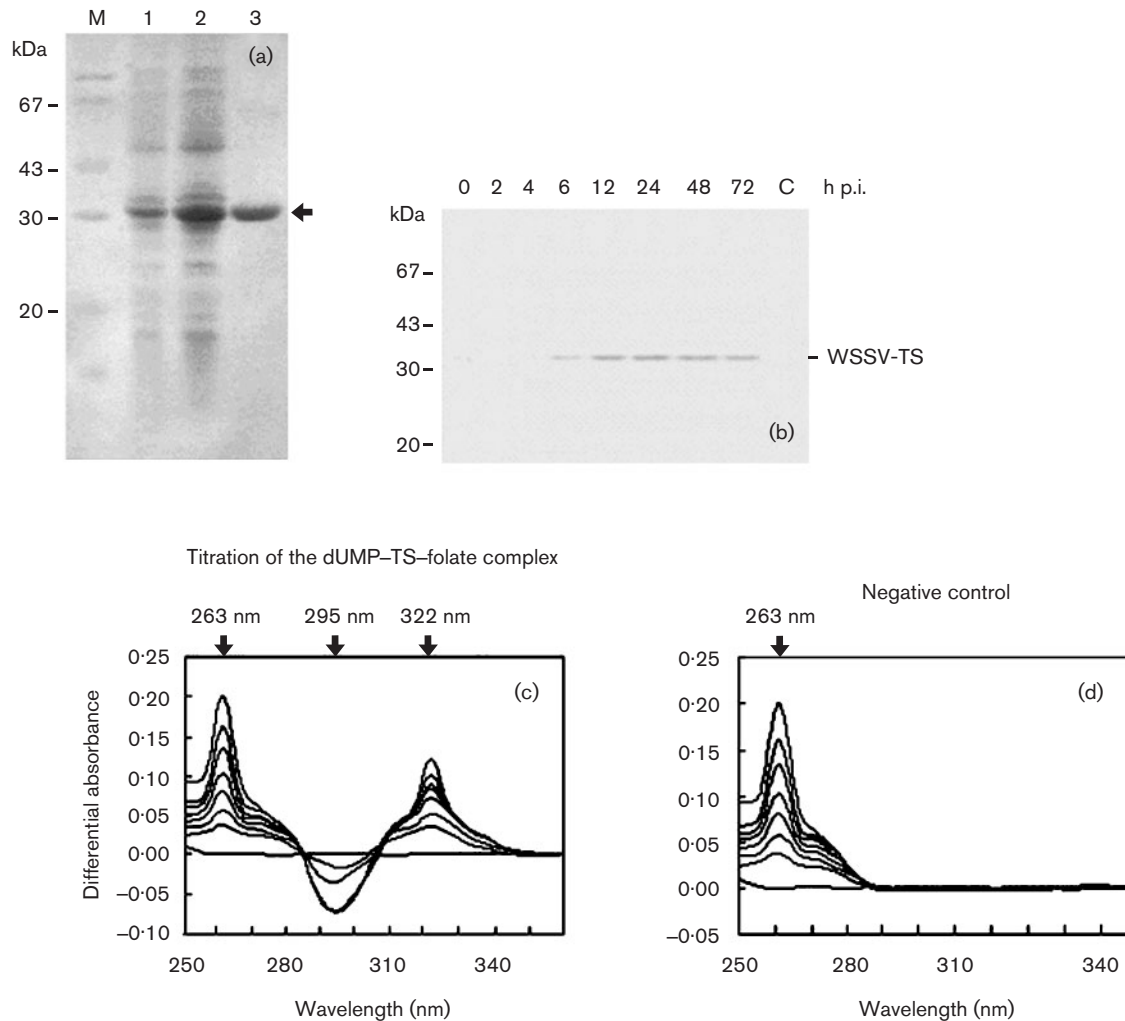


Fig. 4. Western blot analysis and UV difference spectroscopy analysis. (a) The purified *rTS* was detected in a 14% reducing polyacrylamide-SDS gel stained with Coomassie Brilliant blue. Lanes: M, protein molecular mass marker; 1, total soluble protein from bacteria before induction; 2, total soluble protein from bacteria after induction with IPTG; 3, *rTS* purified in the last eluted fraction. (b) Expression analysis of WSSV-TS using Western blotting with antisera against WSSV-TS. The molecular mass is indicated using a protein molecular mass low range marker. (c) The difference spectra shown were obtained by successive addition of dUMP to a sample cuvette containing folate and *rTS* every 1 h, with an equal volume of H₂O added to the reference cuvette. Each addition corresponds to an absorbance increase at ~263 nm and also, prior to saturation at ~322 nm, a decrease at ~295 nm, which represents the dUMP-TS-folate complex. (d) *E. coli* cells were cultured and induced. The final eluate (*rTS*) was used as the negative control. The same amount of dUMP was added to the sample cuvette containing the same buffer and *rTS*. No 322 or 295 nm differences appeared.

1998). By analysing the primary sequence of WSSV-TS, as shown in Fig. 1, the same consensus regions (i.e. containing N²⁰¹, Y²⁰⁵ and D¹⁹³ residues) were also found in WSSV-TS. These highly conserved motifs and residues imply that WSSV-TS has a similar or even the same structure as other TS, and consequently make it possible for it to perform the same biochemical functions.

It has been reported that dUMP binding to, and folate cofactors of, TS cause a major conformational change that converts the enzyme from the open form to a closed form

of the ternary complex and results in spectroscopic changes (Carreras & Santi, 1995) with maximum absorbance at ~330 nm and ~265 nm and minimum absorbance at ~295 nm (Lockshin *et al.*, 1984). UV difference spectroscopic analysis using *rTS* revealed a maximum absorbance at 322 nm and a minimum absorbance at 295 nm, which corresponded to the characteristics of the ternary complex. This presumably reflected changes of chromophores of folate and TS. This difference spectrum suggested that the WSSV-TS protein had the capacity to form a ternary complex in the presence of dUMP and folate.

The TS of WSSV plays a key role in the virus dTTP synthetic system by providing sufficient dTMP for dTTP production. Consequently it has a close relationship with viral DNA replication and proliferation by regulating the balanced supply of dTTP for normal DNA metabolism in collaboration with dUTPase (WSV112), ribonucleotide reductase (WSV172) and thymidylate kinase (WSV395), which are all encoded by the WSSV genome and expressed at the early stage of infection (Tsai *et al.*, 2000; Van Hulten *et al.*, 2000; our unpublished data). The identification of WSSV-TS thus provides us with a new research direction in the prevention and treatment of white spot syndrome disease.

ACKNOWLEDGEMENTS

This work was funded by the National High Technology Research and Development Program (2003AA626020) and Science Fund of State Oceanic Administration (S01301) of China.

REFERENCES

- Adams, M. D., Celniker, S. E., Holt, R. A. & 191 other authors (2000). The genome sequence of *Drosophila melanogaster*. *Science* **287**, 2185–2195.
- Afonso, C. L., Tulman, E. R., Lu, Z., Oma, E., Kutish, G. F. & Rock, D. L. (1999). The genome of *Melanoplus sanguinipes* entomopoxvirus. *J Virol* **73**, 533–552.
- Belfort, M., Maley, G. F., Pedersen-Lane, J. & Maley, F. (1983a). Primary structure of the *Escherichia coli* thyA gene and its thymidylate synthase product. *Proc Natl Acad Sci U S A* **80**, 4914–4918.
- Belfort, M., Moelleken, A., Maley, G. F. & Maley, F. (1983b). Purification and properties of T4 phage thymidylate synthase produced by the cloned gene in an amplification vector. *J Biol Chem* **258**, 2045–2051.
- Beverley, S. M., Ellenberger, T. E. & Cordingley, J. S. (1986). Primary structure of the gene encoding the bifunctional dihydrofolate reductase-thymidylate synthase of *Leishmania major*. *Proc Natl Acad Sci U S A* **83**, 2584–2588.
- Bodemer, W., Niller, H. H., Nitsche, N., Scholz, B. & Fleckenstein, B. (1986). Organization of the thymidylate synthase gene of herpesvirus saimiri. *J Virol* **60**, 114–123.
- Carreras, C. W. & Santi, D. V. (1995). The catalytic mechanism and structure of thymidylate synthase. *Annu Rev Biochem* **64**, 721–762.
- Chen, H. H., Tso, D. J., Yeh, W. B., Cheng, H. J. & Wu, T. F. (2001). The thymidylate synthase gene of Hz-1 virus: a gene captured from its lepidopteran host. *Insect Mol Biol* **10**, 495–503.
- Chen, L. L., Wang, H. C., Huang, C. J. & 9 other authors (2002). Transcriptional analysis of the DNA polymerase gene of shrimp white spot syndrome virus. *Virology* **301**, 136–147.
- Cheng, Q. & Saul, A. (1994). The dihydrofolate reductase domain of rodent malaria: point mutations and pyrimethamine resistance. *Mol Biochem Parasitol* **65**, 361–363.
- Chiericatti, G. & Santi, D. V. (1998). Aspartate 221 of thymidylate synthase is involved in folate cofactor binding and in catalysis. *Biochemistry* **37**, 9038–9042.
- Cox, K. M., Robertson, D. & Fites, R. C. (1999). Mapping and expression of a bifunctional thymidylate synthase, dihydrofolate reductase gene from maize. *Plant Mol Biol* **41**, 733–739.
- Danenberg, P. V. (1977). Thymidylate synthetase – a target enzyme in cancer chemotherapy. *Biochim Biophys Acta* **473**, 73–92.
- Davison, A. J. & Scott, J. E. (1986). The complete DNA sequence of varicella-zoster virus. *J Gen Virol* **67**, 1759–1816.
- Eastwood, D. C., Bains, N. K., Henderson, J. & Burton, K. S. (2000). Genomic sequencing of superoxide dismutase in *Agaricus bisporus*. Submitted to the EMBL/GenBank/DBJ databases.
- Edgell, D. R. & Shub, D. A. (2001). Related homing endonucleases I-BmoI and I-TevI use different strategies to cleave homologous recognition sites. *Proc Natl Acad Sci U S A* **98**, 7898–7903.
- Eldin de Pecoulas, P., Basco, L. K., Tahar, R., Ouatas, T. & Mazabraud, A. (1998). Analysis of the *Plasmodium vivax* dihydrofolate reductase-thymidylate synthase gene sequence. *Gene* **211**, 177–185.
- Gamarro, F., Yu, P. L., Zhao, J., Edman, U., Greene, P. J. & Santi, D. (1995). *Trypanosoma brucei* dihydrofolate reductase-thymidylate synthase gene isolation and expression and characterization of the enzyme. *Mol Biochem Parasitol* **72**, 11–22.
- Hardy, L. W. & Nalivaika, E. (1992). Asn¹⁷⁷ in *Escherichia coli* thymidylate synthase is a major determinant of pyrimidine specificity. *Proc Natl Acad Sci U S A* **89**, 9725–9729.
- Honess, R. W., Bodemer, W., Cameron, K. R., Niller, H. H., Fleckenstein, B. & Randall, R. E. (1986). The A-rich genome of herpesvirus saimiri contains a highly conserved gene for thymidylate synthase. *Proc Natl Acad Sci U S A* **83**, 3604–3608.
- Huang, C., Zhang, X., Lin, Q., Xu, X., Hu, Z. & Hew, C. L. (2002). Proteomic analysis of shrimp white spot syndrome viral proteins and characterization of a novel envelope protein VP466. *Mol Cell Proteomics* **1**, 223–231.
- Hughes, D. E., Shonekan, O. A. & Simpson, L. (1989). Structure, genomic organization and transcription of the bifunctional dihydrofolate reductase-thymidylate synthase gene from *Crithidia fasciculata*. *Mol Biochem Parasitol* **34**, 155–166.
- Ivanova, N., Anderson, I., Bhattacharyya, A. & 16 other authors (2002). The genome sequence of the facultative intracellular pathogen *Brucella melitensis*. *Proc Natl Acad Sci U S A* **99**, 443–448.
- Ivanova, N., Sorokin, A., Anderson, I. & 20 other authors (2003). Genome sequence of *Bacillus cereus* and comparative analysis with *Bacillus anthracis*. *Nature* **423**, 87–91.
- Kaneda, S., Nalbantoglu, J., Takeishi, K., Shimizu, K., Gotoh, O., Seno, T. & Ayusawa, D. (1990). Structural and functional analysis of the human thymidylate synthase gene. *J Biol Chem* **265**, 20277–20284.
- Kenny, E., Atkinson, T. & Hartley, B. S. (1985). Nucleotide sequence of the thymidylate synthetase gene (thyP3) from the *Bacillus subtilis* phage phi 3T. *Gene* **34**, 335–342.
- Kozak, M. (1989). The scanning model for translation: an update. *J Cell Biol* **108**, 229–234.
- Lockshin, A., Mondal, K. & Danenberg, P. V. (1984). Spectroscopic studies of ternary complexes of thymidylate synthase, deoxyribonucleotides, and folate analogs. *J Biol Chem* **259**, 11346–11352.
- Luo, M., Piffanelli, P., Rastelli, L. & Cella, R. (1993). Molecular cloning and analysis of a cDNA coding for the bifunctional dihydrofolate reductase-thymidylate synthase of *Daucus carota*. *Plant Mol Biol* **22**, 427–435.
- McLauchlan, J., Gaffney, D., Whitton, J. L. & Clements, J. B. (1985). The consensus sequence YGIGTTY located downstream from the AATAAA signal is required for efficient formation of mRNA 3' termini. *Nucleic Acids Res* **13**, 1347–1368.
- Muller, K., Tidona, C. A., Bahr, U. & Darai, G. (1998). Identification of a thymidylate synthase gene within the genome of Chilo iridescent virus. *Virus Genes* **17**, 243–258.

- Nelson, K., Alonso, G., Langer, P. J. & Beverley, S. M. (1990). Sequence of the dihydrofolate reductase-thymidylate synthase (DHFR-TS) gene of *Leishmania amazonensis*. *Nucleic Acids Res* **18**, 2819.
- Nierman, W. C., Feldblyum, T. V., Laub, M. T. & 34 other authors (2001). Complete genome sequence of *Caulobacter crescentus*. *Proc Natl Acad Sci U S A* **98**, 4136–4141.
- Nishio, Y., Nakamura, Y., Kawarabayasi, Y. & 8 other authors (2003). Comparative complete genome sequence analysis of the amino acid replacements responsible for the thermostability of *Corynebacterium efficiens*. *Genome Res* **13**, 1572–1579.
- Noelling, J., Breton, G., Omelchenko, M. V. & 16 other authors (2001). Genome sequence and comparative analysis of the solvent-producing bacterium *Clostridium acetobutylicum*. *J Bacteriol* **183**, 4823–4838.
- Perry, K. M., Fauman, E. B., Finer-Moore, J. S., Montfort, W. R., Maley, G. F., Maley, F. & Stroud, R. M. (1990). Plastic adaptation toward mutations in proteins: structural comparison of thymidylate synthases. *Proteins* **8**, 315–333.
- Perryman, S. M., Rossana, C., Deng, T. L., Vanin, E. F. & Johnson, L. F. (1986). Sequence of a cDNA for mouse thymidylate synthase reveals striking similarity with the prokaryotic enzyme. *Mol Biol Evol* **3**, 313–321.
- Read, T. D., Peterson, S. N., Tourasse, N. & 49 other authors (2003). The genome sequence of *Bacillus anthracis* Ames and comparison to closely related bacteria. *Nature* **423**, 81–86.
- Reche, P., Arrebola, R., Olmo, A., Santi, D. V., Gonzalez-Pacanowska, D. & Ruiz-Perez, L. M. (1994). Cloning and expression of the dihydrofolate reductase-thymidylate synthase gene from *Trypanosoma cruzi*. *Mol Biochem Parasitol* **65**, 247–258.
- Richter, J., Puchtler, I. & Fleckenstein, B. (1988). Thymidylate synthase gene of herpesvirus atelae. *J Virol* **62**, 3530–3535.
- Roos, D. S. (1993). Primary structure of the dihydrofolate reductase-thymidylate synthase gene from *Toxoplasma gondii*. *J Biol Chem* **268**, 6269–6280.
- Russo, J. J., Bohenzky, R. A., Chien, M. C. & 8 other authors (1996). Nucleotide sequence of the Kaposi sarcoma-associated herpesvirus (HHV8). *Proc Natl Acad Sci U S A* **93**, 14862–14867.
- Schiffer, C. A., Clifton, I. J., Davisson, V. J., Santi, D. V. & Stroud, R. M. (1995). The crystal structure of human thymidylate synthase: a structural mechanism for guiding substrates into the active site. *Biochemistry* **34**, 16279–16287.
- Schlichtherle, I. M., van Houten, J. L. & Roos, D. S. (1996). Cloning and molecular analysis of the bifunctional dihydrofolate reductase-thymidylate synthase gene in the ciliated protozoan *Paramecium tetraurelia*. *Mol Genet Gen* **250**, 665–673.
- Shigenobu, S., Watanabe, H., Hattori, M., Sakaki, Y. & Ishikawa, H. (2000). Genome sequence of the endocellular bacterial symbiont of aphids *Buchnera* sp. APS. *Nature* **407**, 81–86.
- Singer, S. C., Richards, C. A., Ferone, R., Benedict, D. & Ray, P. (1989). Cloning, purification, and properties of *Candida albicans* thymidylate synthase. *J Bacteriol* **171**, 1372–1378.
- Tamas, I., Klasson, L., Canbaeck, B., Naeslund, A. K., Eriksson, A. S., Wernegreen, J. J., Sandstroem, J. P., Moran, N. A. & Andersson, S. G. E. (2002). 50 million years of genomic stasis in endosymbiotic bacteria. *Science* **296**, 2376–2379.
- Taylor, G. R., Lagosky, P. A., Storms, R. K. & Haynes, R. H. (1987). Molecular characterization of the cell cycle-regulated thymidylate synthase gene of *Saccharomyces cerevisiae*. *J Biol Chem* **262**, 5298–5307.
- Telford, E. A. R., Watson, M. S., Aird, H. C., Perry, J. & Davison, A. J. (1995). The DNA sequence of equine herpesvirus 2. *J Mol Biol* **249**, 520–528.
- Tian, L. & Tam, J. W. O. (1998). Molecular cloning of thymidylate synthase from *Ascaris suum*. Submitted to the EMBL/GenBank/DDDBJ databases.
- Tong, Y. (1998). Thymidylate synthase (TS) that contain single residue substitutions within the highly conserved Arg50-loop, which binds the pyrimidine substrate. *J Biol Chem* **273**, 11611–11618.
- Tsai, M. F., Yu, H. T., Tzeng, H. F. & 7 other authors (2000). Identification and characterization of a shrimp white spot syndrome virus (WSSV) gene that encodes a novel chimeric polypeptide of cellular-type thymidine kinase and thymidylate kinase. *Virology* **277**, 100–110.
- Van Dijk, M. R., McConkey, G. A., Vinkenoog, R., Waters, A. P. & Janse, C. J. (1994). Mechanisms of pyrimethamine resistance in two different strains of *Plasmodium berghei*. *Mol Biochem Parasitol* **68**, 167–171.
- Van Ham, R. C. H. J., Kamerbeek, J., Palacios, C. & 13 other authors (2003). Reductive genome evolution in *Buchnera aphidicola*. *Proc Natl Acad Sci U S A* **100**, 581–586.
- Van Hulten, M. C. W., Tsai, M. F., Schipper, C. A., Lo, C. F., Kou, G. H. & Vlak, J. M. (2000). Analysis of a genomic segment of white spot syndrome virus of shrimp containing ribonucleotide reductase genes and repeat regions. *J Gen Virol* **81**, 307–316.
- Van Hulten, M. C. W., Wittenberg, M., Goodall, S. D. & Vlak, J. M. (2001). Identification of two major virion protein genes of white spot syndrome virus of shrimp. *Virology* **266**, 227–236.
- Wang, M., Ratnam, S. & Freisheim, J. H. (1995). Cloning, nucleotide sequence and expression of the bifunctional dihydrofolate reductase-thymidylate synthase from *Glycine max*. *Biochim Biophys Acta* **1261**, 325–336.
- Yang, F., He, J., Lin, X., Li, Q., Pan, D., Zhang, X. & Xu, X. (2001). Complete genome sequence of the shrimp white spot syndrome virus. *J Virol* **75**, 11811–11820.
- Zhang, X., Huang, C., Xu, X. & Hew, C. L. (2002). Transcription and identification of an envelope protein gene (p22) from shrimp white spot syndrome virus. *J Gen Virol* **83**, 471–477.